

## NONLINEAR MODELING AND ANALYSIS OF POWER LINES WITH STOCKBRIDGE DAMPERS UNDER VORTEX-INDUCED VIBRATIONS

**Arun L Malla, Sunit K Gupta**

Department of Mechanical Engineering  
Virginia Polytechnic Institute and State University  
Blacksburg, Virginia 24061

**Oumar Barry \***

Department of Mechanical Engineering  
Virginia Polytechnic Institute and State University  
Blacksburg, Virginia 24061  
Email: obarry@vt.edu

### ABSTRACT

Vortex-induced vibrations have a considerable effect on overhead power transmission lines, often leading to fatigue-failure. While nonlinear models exist for power lines, vibration dampers, and vortex-induced vibrations, no work combines the nonlinearities stemming from the cable, vibration damper, and fluid forces in a single model. As power transmission lines are a major component of modern infrastructure, a thorough understanding of the nonlinear dynamic interactions of conductors, dampers, and wind forces is crucial. This paper examines a conductor with attached Stockbridge dampers under vortex-induced vibration. Sources of nonlinearity in this system include mid-plane stretching of the conductor, equivalent cubic stiffness of the Stockbridge damper, and fluctuating lift force modeled as a Van der Pol oscillator. The equations of motion for the resulting system are discretized using Galerkin's method and solved using the numerical continuation method. Through parametric analysis, the effects of factors such as damper position and mass ratio on system response are determined. Insight is gained on the combined nonlinear system and a strong foundation is formed for ongoing study.

### INTRODUCTION

Wind-induced vibrations are a major factor in the fatigue failure of overhead power transmission lines, or con-

ductors. One specific type of wind-induced vibrations is aeolian vibrations. Aeolian vibrations are driven by periodic vortex shedding that occurs due to cross-flow past a bluff cylindrical body [1]. They are caused by wind speeds of 1–7 m/s, and consist of relatively low amplitude and high frequency vibrations [2–5]. As a power line undergoes Aeolian vibration, fatigue damage accumulates on its clamped ends, potentially leading to failure. To prevent this failure, vibrations can be mitigated by installing Stockbridge dampers on the conductors near the clamps at either end [6].

The effect of aeolian vibrations on conductors with dampers or other in-span fittings has been previously studied using several methods. These include the energy balance method [7–10] and impedance method [11–13]. The conductor has been modeled as a cable or Euler-Bernoulli beam, while Stockbridge dampers have been modeled as a concentrated force, another Euler-Bernoulli beam, or an equivalent mass-spring-damper-mass system. Even setting aside the vortex-induced forcing, there are multiple sources of nonlinearity in this system. From the attached damper, there is a cubic nonlinearity from the spring-mass system. From the conductor itself, nonlinearity stems from mid-plane stretching of a beam with fixed ends. Dowell's model of a nonlinear beam with spring-mass system included the former nonlinearity [14], and was expanded by Pakdemirli and Nayfeh to add the latter [15]. This model was expanded to include axial tension and multiple mass-spring-damper systems by Barry et al [16], and further extended to include

\*Address all correspondence to this author.

a wind-induced forcing term by Bukhari [17].

In previous works, the vortex-induced wind forces were commonly represented by a single excitation term [6] or determined from experimental data [9]. However, vortex-induced vibrations are significantly nonlinear and have been the subject of numerous studies on their own. This body of work has been extensively reviewed by Sarpkaya [18], Griffin and Ramberg [19], Parkinson [20], and Pantazopolous [21]. One notable trait of vortex-induced forces is the lock-in condition. Through experiments, it has been shown that the vortex shedding frequency locks on to a flexible structure's natural frequency in a phenomenon known as lock-in or synchronization. This leads to resonance of vortex-induced vibrations, increasing the vortex strength and fluid forces [22].

These fluid forces can be divided into cross-flow and in-line components oriented perpendicular and parallel to flow direction respectively. Studies on the response of cylindrical structures within fluid flow tend to focus on the cross-flow response because in-line motions are often an order of magnitude smaller than cross-flow response [22]. There have been numerous models developed to analyze cross-flow response, both analytical and numerical. Because of similarities with the vortex shedding process, a number of these models use equations of nonlinear oscillators such as the Van der Pol oscillator to represent the fluctuating cross-flow (lift) force on the structure [23–25]. These models proved successful in identifying the controlling factor [24, 25] and modal scaling principle [26, 27] in a structure's response. Following these conventions, this work takes into account the lift force only, utilizing a model based on the Van der Pol oscillator as detailed by Skop and Balasubramanian [1].

In this paper, this nonlinear model of lift force is coupled for the first time with the nonlinear beam-damper system previously described. The conductor is modeled as an Euler-Bernoulli beam with a number of attached mass-spring-damper systems. Forces on the conductor include pretension and the vortex-induced lift force. Sources of nonlinearity in this model include mid-plane stretching, cubic spring stiffness, and the fluctuation of the lift force. Using this model, the numerical continuation method is employed to determine the conductor's frequency-amplitude relation for the lock-in case of primary resonance near the system's fundamental natural frequency. These results are validated through comparison to prior literature and an alternate numerical method, then used in parametric studies to determine the effect of selected parameters on system response.

## MATHEMATICAL FORMULATION

A schematic of a single conductor with a pair of attached Stockbridge dampers is shown in Fig. 1. Here, the conductor is represented by an Euler-Bernoulli beam and

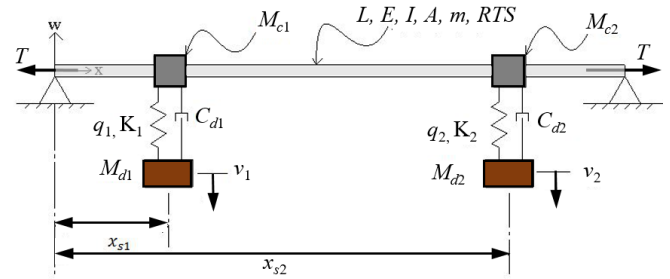


Figure 1: Schematic of a transmission cable with attached nonlinear vibration absorbers.

the Stockbridge attachments are reduced to mass-spring-damper-mass systems with equivalent properties. In this model, the beam has length  $L$ , flexural rigidity  $EI$ , axial rigidity  $EA$ , mass per unit length  $m$ , and diameter  $D$ . Each equivalent damper  $p$  has in-span mass  $M_{cp}$ , suspended mass  $M_{dp}$ , linear stiffness  $K_p$ , cubic nonlinear stiffness  $q_p$ , and dashpot damping coefficient  $C_{dp}$ . Its position along the beam from the left-end reference frame is denoted  $x_{sp}$ . The beam is also subject to a pretension  $T$  and fluctuating lift force  $F_L$ . The surrounding fluid flows perpendicular to the beam's axis at a velocity of  $V_f$ , and has a density  $\rho_f$ .

For this system, the beam's axial coordinate is denoted by  $x$ , the cross-flow (transverse) beam displacement is denoted by  $W(x, t)$  and the displacement of  $M_{dp}$  is denoted by  $V_p(t)$ . The number of attached dampers is denoted as  $n$ . The notations dot ( $\dot{\phantom{x}}$ ) and prime ( $\prime$ ) represent temporal and spatial derivatives, respectively.

After expressing the Lagrangian and applying Hamilton's principle for an Euler-Bernoulli beam, the nonlinear equations of motion and boundary conditions for this system can be written as:

$$m\ddot{W} + EIW^{iv} - TW'' = \frac{EA - T}{2L} \int_0^L W'^2 dx W'' - 2\mu\dot{W} + F_L + \sum_{p=1}^n \left[ M_{cp}\ddot{W} + K_p(W - V_p) + q_p(W - V_p)^3 + C_{dp}(\dot{W} - \dot{V}_p) \right] \delta(x - x_{sp}) \quad (1)$$

$$W(0, t) = 0 \quad (2)$$

$$W''(0, t) = 0 \quad (3)$$

$$W(L, t) = 0 \quad (4)$$

$$W''(L, t) = 0 \quad (5)$$

$$M_{dp}\ddot{V}_p(t) = K_p(W_p(x_{sp}, t) - V_p(t)) + q_p(W_p(x_{sp}, t) - V_p(t))^3 + C_{dp}(\dot{W}_p(x_{sp}, t) - \dot{V}_p(t)) \quad (6)$$

where  $p = 1, 2, \dots, n$ .

In Eq. (1),  $\mu$  is the internal damping coefficient and  $F_L(x, t)$  is the fluctuating fluid force across the conductor. Following Perkins [22],  $F_L$  can be defined in terms of fluctuating lift coefficient  $C_L(x, t)$  as:

$$F_L(x, t) = \frac{\rho_f V_f^2 D C_L(x, t)}{2} \quad (7)$$

Here,  $C_L$  is defined by two terms: an excitation  $Q(x, t)$  that stems from the response of the conductor and a stall term. This stall term, shown in Eq. (8), enforces a self-limiting response for all system parameter values.

$$C_L(x, t) = Q(x, t) - \frac{2\alpha}{\omega_s} \dot{W}(x, t) \quad (8)$$

where  $\omega_s$  is the vortex shedding frequency. Due to the lock-in condition, it can be assumed that  $\omega_s \cong \omega_{n,j}$ , where  $\omega_{n,j}$  is the  $j^{\text{th}}$  natural frequency for the conductor response.

Following Skop and Balasubramanian [1], the excitation term  $Q(x, t)$  is modelled by a Van der Pol equation:

$$\ddot{Q} - \omega_s G (C_{L0}^2 - 4Q^2) \dot{Q} + \omega_s^2 Q = \omega_s F \dot{W} \quad (9)$$

Here,  $G$  and  $F$  are constant parameters determined from experimental data, and  $C_{L0}$  is the lift coefficient for a stationary cylinder.

For convenience, the above equations are nondimensionalized using the following substitutions of dimensionless variables:

$$\begin{aligned} \xi &= \frac{x}{L}; & \xi_p &= \frac{x_{sp}}{L}; & w &= \frac{W}{r}; \\ v_p &= \frac{V_p}{r}; & \tau &= \frac{t}{L^2} \sqrt{\frac{EI}{m}} \end{aligned} \quad (10)$$

Substituting Eq. (10) into Eqs. (1)–(9) provides nondimensional equations:

$$\begin{aligned} \ddot{w} + w^{iv} - 2s^2 w'' &= \frac{\lambda}{2} \int_0^1 w'^2 d\xi w'' - 2\bar{\mu} \dot{w} + f_L \left( q \right. \\ &\quad \left. - \frac{2\bar{\alpha}}{\bar{\omega}_s} \dot{w} \right) + \sum_{p=1}^n \left[ \alpha_{1p} \ddot{w} + k_p (w - v_p) \right. \\ &\quad \left. + \gamma_p (w - v_p)^3 + c_{dp} (\dot{w} - \dot{v}_p) \right] \delta(\xi - \xi_{sp}) \end{aligned} \quad (11)$$

$$w(0, \tau) = 0 \quad (12)$$

$$w''(0, \tau) = 0 \quad (13)$$

$$w(L, \tau) = 0 \quad (14)$$

$$w''(L, \tau) = 0 \quad (15)$$

$$\begin{aligned} \alpha_{2p} \ddot{v}_p(\tau) &= k_p (w_p(\xi_p, \tau) - v_p(\tau)) + \gamma_p (w_p(\xi_p, \tau) - v_p(\tau))^3 \\ &\quad + c_{dp} (\dot{w}_p(\xi_p, \tau) - \dot{v}_p(\tau)) \end{aligned} \quad (16)$$

$$\ddot{q} - \bar{\omega}_s G (C_{L0}^2 - 4q^2) \dot{q} + \bar{\omega}_s^2 q = \bar{\omega}_s \bar{F} \dot{w} \quad (17)$$

where:

$$\begin{aligned} s &= \sqrt{\frac{TL^2}{2EI}}; & \lambda &= 1 - 2s^2 \frac{r^2}{L^2}; & \bar{\mu} &= \mu \frac{L^4}{EI r}; \\ f_L &= \frac{L^4 \rho_f V_f^2 D}{2EI r}; & \alpha_{1p} &= \frac{M_{cp}}{mL}; & \alpha_{2p} &= \frac{M_{dp}}{mL}; \\ k_p &= \frac{K_p L^3}{EI}; & \gamma_p &= \frac{q_p L^3 r^2}{EI}; & c_{dp} &= \frac{C_{dp} L^2}{M_{dp}} \sqrt{\frac{m}{EI}}; \\ \bar{\alpha} &= \alpha r; & \bar{F} &= Fr; & \bar{\omega}_s &= \omega_s \sqrt{\frac{mL^4}{EI}} \end{aligned} \quad (18)$$

The conductor response  $w$  and excitation term  $q$  have modal expansions:  $w(\xi, \tau) = \sum Y_j(\xi) \bar{w}_j(\tau)$  and  $q(\xi, \tau) = \sum Y_j(\xi) \bar{q}_j(\tau)$ . From the experimental work of Ramberg and Griffin, it has been demonstrated that a vortex-induced excitation shares the normal modes of the conductor response, i.e. their mode shapes  $Y_j(\xi)$  are identical [28, 29].

### Galerkin's Method

To discretize these partial differential equations, an assumed mode shape that satisfies the boundary conditions is used to approximate  $w$  and  $q$ . This approximate mode shape is:

$$Y_j(\xi) = \sin(j\pi\xi) \quad (19)$$

Thus:

$$w = \sum_{j=1}^{\infty} \bar{w}_j \sin(j\pi\xi) \quad (20)$$

$$q = \sum_{j=1}^{\infty} \bar{q}_j \sin(j\pi\xi) \quad (21)$$

Once these approximations are substituted into Eqs. (11), (16), and (17), equality will no longer be satisfied. This results in an error term for each equation,  $\epsilon_i$ , where  $i = 1 - 3$ . For instance, from Eq. (11):

$$\begin{aligned} \epsilon_1 &= \ddot{w} + w^{iv} - 2s^2 w'' - \frac{\lambda}{2} \int_0^1 w'^2 d\xi w'' + 2\bar{\mu} \dot{w} \\ &\quad - f_L \left( q - \frac{2\bar{\alpha}}{\bar{\omega}_s} \dot{w} \right) - \sum_{p=1}^n \left[ \alpha_{1p} \ddot{w} + k_p (w - v_p) \right. \\ &\quad \left. + \gamma_p (w - v_p)^3 + c_{dp} (\dot{w} - \dot{v}_p) \right] \delta(\xi - \xi_{sp}) \end{aligned} \quad (22)$$

Thus, the the values  $\bar{w}_j$  and  $\bar{q}_j$  that satisfy this system can be determined by setting the weighted integral of each error expression equal to zero. These weighted integrals are

formed using the mode shapes  $Y_k$  as weighting functions and integrating over the length of the beam, yielding:

$$\int_0^L \epsilon_i Y_k d\xi = 0 \quad (23)$$

By obtaining the three error functions, substituting into Eq. (23), and integrating, the system of partial differential equations in  $\xi$  and  $\tau$  can be transformed into a set of ordinary differential equations that depend solely on  $\tau$ . For a system with a single Stockbridge damper ( $n = 1$ ), this yields the equations:

$$\begin{aligned} & \ddot{w} + 2\alpha_1 s_j^2 \ddot{w} + j^4 \pi^4 \bar{w} + 2j^2 \pi^2 s^2 \bar{w} \\ & + \frac{\lambda}{4} j^2 \pi^2 s_j^2 \bar{w} + f_L \frac{2\bar{\alpha}}{\bar{\omega}_s} \dot{w} - f_L \bar{q} + 2\bar{\mu} \dot{w} \\ & + 2c_d s_j^2 \dot{w} - 2c_d s_j \dot{v} + 2k s_j^2 \bar{w} - 2k s_j v + 2\gamma v^3 s_j \\ & + 2\gamma s_j^4 \bar{w}^3 + 6\gamma s_j^2 v^2 \bar{w} - 6\gamma s_j^3 v \bar{w}^2 = 0 \end{aligned} \quad (24)$$

$$\begin{aligned} & \alpha_2 \ddot{v} + c_d \dot{v} + kv + \gamma v^3 - \gamma \bar{w}^3 s_j^3 - c_d s_j \dot{w} \\ & - k s_j \bar{w} - 3\gamma s_j v^2 \bar{w} + 3\gamma s_j^2 v \bar{w}^2 = 0 \end{aligned} \quad (25)$$

$$\ddot{q} - \bar{\omega}_s G \left( C_{L0}^2 - 3\bar{q}^2 \right) \dot{q} + \bar{\omega}_s^2 \bar{q} - \bar{\omega}_s \bar{F} \dot{w} = 0 \quad (26)$$

where  $s_j = \sin(j\pi\xi_s)$ .

Skop and Iwan have demonstrated that when  $\omega_s \cong \omega_{n,j}$ , only the  $j^{th}$  mode significantly contributes to the modal expansion of  $q(\xi, \tau)$  [26, 27]. Perkins also showed that for  $\omega_s \cong \omega_{n,j}$ , the only forced component of the conductor response  $w(\xi, \tau)$  is the  $j^{th}$  mode. Since this study focuses on the case of lock-in and primary resonance near the fundamental natural frequency, only the first mode shape,  $j = 1$ , of the system will be analyzed moving forward.

The system of nonlinear differential equations (24)–(26) serves as a model for the conductor-damper system under wind-induced vibrations. The numerical continuation method was used to determine this system's frequency-amplitude relations.

## VALIDATION

Two factors were used to validate the continuation method. The first five natural frequencies were determined and compared against previous literature, and the system's steady-state response was determined and compared to a numerical solution using the MATLAB routine ode45.

Through simulating the system without forcing or damping until steady state, the first several natural frequencies of the cable were found. These were compared to previous works that studied similar systems using the method of multiple scales [17] and finite element analysis [5].

Table 1: Validation of natural frequencies (Hz) for a conductor with single damper.  $\xi_s = 0.05$ ,  $\alpha_1 = 0.0045$ ,  $\alpha_2 = 0.1088$ ,  $s = 80.33$ ,  $k = 17139.7$

Study	$\omega_{n,1}$	$\omega_{n,2}$	$\omega_{n,3}$	$\omega_{n,4}$	$\omega_{n,5}$
Present	2.3950	2.6677	4.7941	7.2143	9.6343
Multiple Scales [17]	2.3634	2.6366	4.8244	7.2402	9.6696
FEA [5]	2.3845	2.6387	4.8164	7.2337	9.6663

As shown in Table 1, there is high agreement between four of the first five natural frequencies. The first, third, fourth and fifth frequencies are those of the conductor, while the second is the natural frequency of the damper. This comparison indicates that the utilized methods are valid, giving confidence to the following analysis.

To further validate the results of the continuation method, the steady-state response obtained by continuation was compared to the direct numerical solution using MATLAB's ode45 routine. Fig. 2 displays very good agreement between the phase portraits of these two solutions at the same excitation frequency.

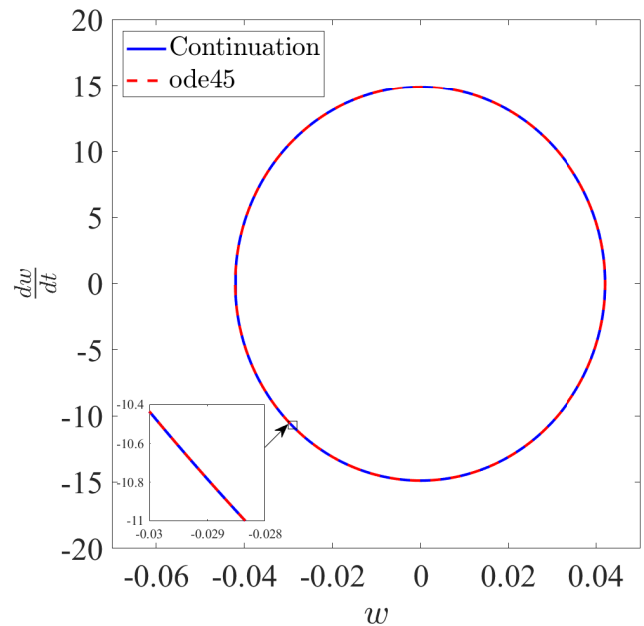


Figure 2: Phase portrait validation of steady-state conductor response.

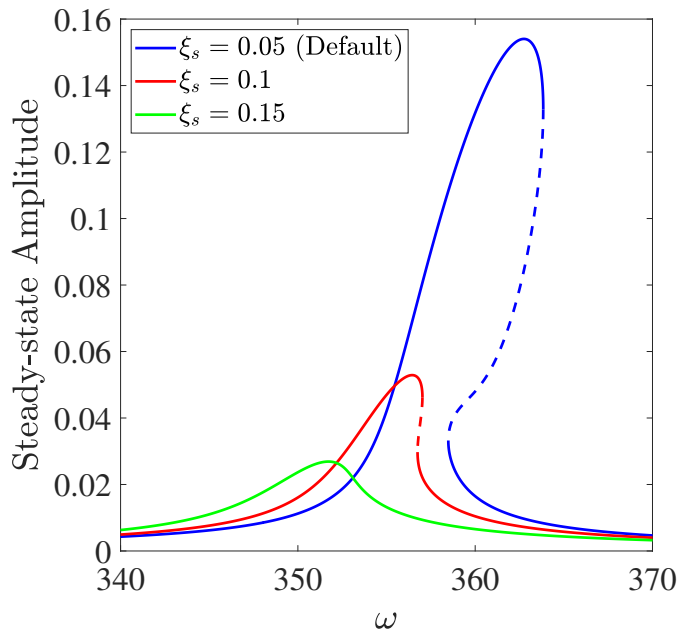


Figure 3: Vibration amplitude versus nonlinear frequency for varied values of  $\xi_s$ .

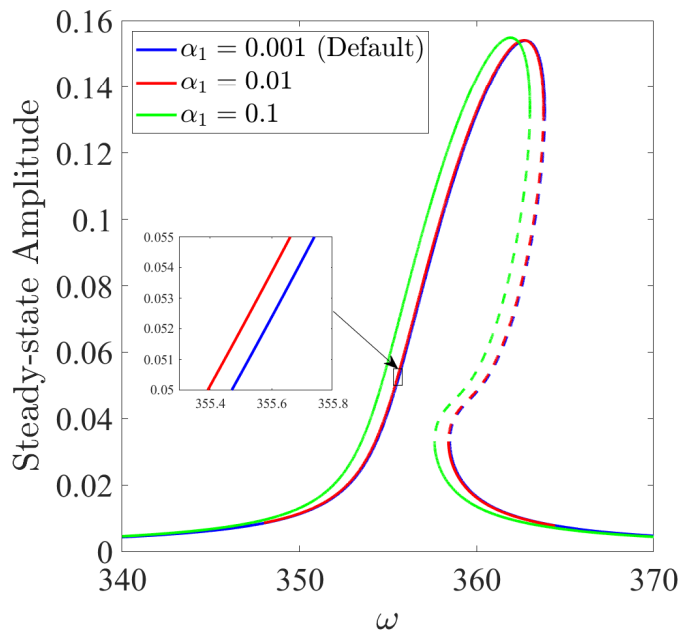


Figure 4: Vibration amplitude versus nonlinear frequency for varied values of  $\alpha_1$ .

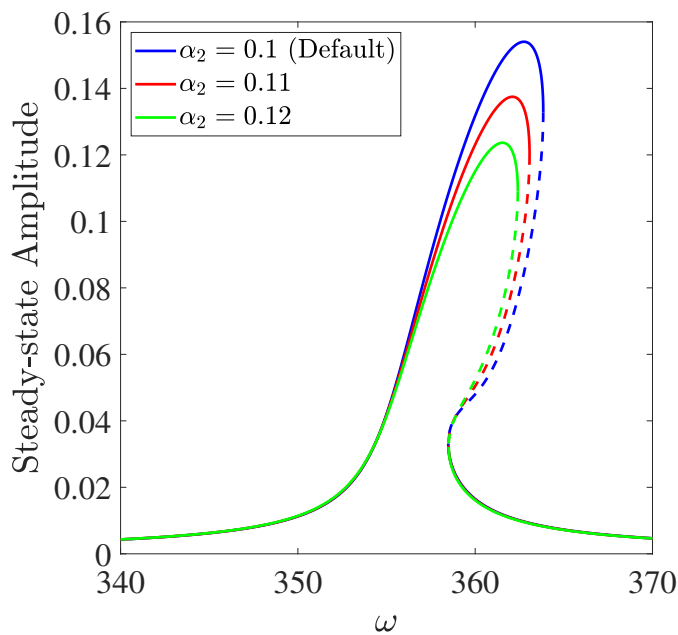


Figure 5: Vibration amplitude versus nonlinear frequency for varied values of  $\alpha_2$ .

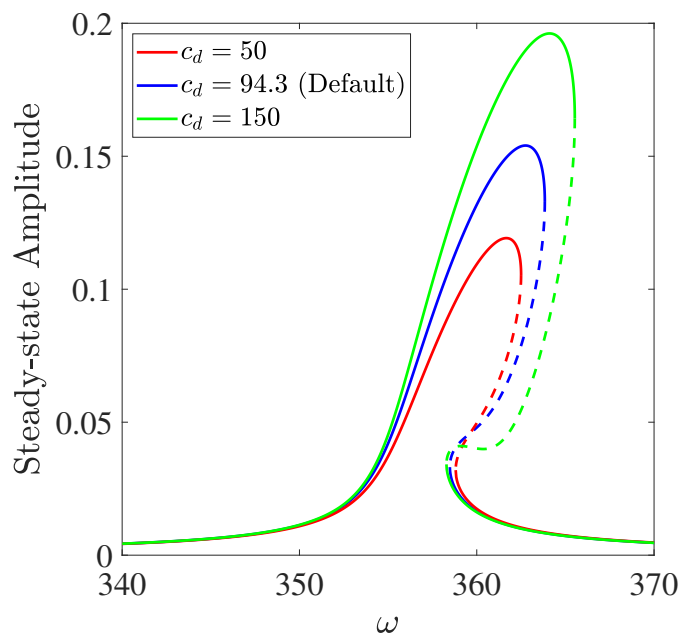


Figure 6: Vibration amplitude versus nonlinear frequency for varied values of  $c_d$ .

### PARAMETRIC ANALYSIS

To build understanding of the coupled system, the response of the conductor was examined. Four parameters were varied to determine their effect on the conductor's

nonlinear frequency-amplitude relation. These parameters were: damper position  $\xi_s$ , in-span mass ratio  $\alpha_1$ , hanging mass ratio  $\alpha_2$ , and dashpot damping coefficient  $c_d$ . In all

cases, the default parameters were:  $\xi_s = 0.05$ ,  $\alpha_1 = 0.001$ ,  $\alpha_2 = 0.1$ ,  $c_d = 94.3$ ,  $s = 80.33$ ,  $k = 17139.7$ ,  $\gamma = 0.1$ ,  $\bar{\mu} = 0.2$ ,  $f_L = 148.1$ ,  $\alpha = 0.183$ ,  $F = 1.0027$ ,  $G = 0.3763$ . Only one parameter was varied for each simulation. In all figures, solid lines indicate a curve's stable region while dashed lines indicate the unstable region, if present.

In Fig. 3, the influence of damper position  $\xi_s$  is illustrated. Through numerical simulation, it was determined that the sine mode shape was not valid for all positions of  $\xi_s$ ; at higher values, this approximation began to break down. Furthermore, Stockbridge dampers are usually placed near the conductor ends, as galloping can cause early fatigue failure for dampers placed further from the ends of the conductor [30,31]. For both of these reasons,  $\xi_s$  was varied from 0.05–0.15. As the damper position moves away from the clamped end, the conductor's vibration amplitude decreased. This indicates improved performance of the damper as it moves away from the node at the conductor end and closer to the vibration antinode at the conductor midpoint. Additionally, it can be seen that as the amplitude decreases, the effect of nonlinearity on the system decreases.

Fig. 4 shows that increasing the in-span damper mass  $\alpha_1$  from 0.001 to 0.01 has a minimal effect on the conductor vibration. Altering this mass by another factor of 10 to 0.1, the system's nonlinear frequency visibly decreases, but there is still little effect on the nonlinearity of the system, and a very slight increase in the amplitude of the response. The shift in frequency is logical, as placing or increasing an in-span mass on a beam is known to affect the system's natural frequency. Regarding the effect of this mass ratio on nonlinearity, there is the potential of greater effect if  $\alpha_1$  is increased further. However, the presence of an increased in-span mass would result in further effects on the system's natural frequency as well as increased vibration amplitude, which could adversely affect the system.

In addition, the bulk of mass in a Stockbridge damper (i.e., ratio of the hanging mass over the total mass of the cable,  $\alpha_2$ ) has a much more significant effect on the vibration amplitude, as can be seen in Fig. 5. Increasing  $\alpha_2$  in increments of 0.01 significantly impacts the vibration amplitude; even this relatively small change in hanging mass displays increased damper effectiveness. Nonlinearity does not visibly change with this small variation in hanging mass, but a larger range of  $\alpha_2$  could change this observation. However, similarly to the effect of increasing  $\xi_s$ , some values of  $\alpha_2$  were found to make the sine approximation of the mode shape inaccurate, restricting the range of the current study.

In contrast, increasing the dashpot damping  $c_d$  results in increased vibration amplitude but decreased effect of nonlinearity, illustrated in Fig. 6. This indicates that a Stockbridge damper with higher dashpot damping will actually be less effective at absorbing the vibration of the conductor,

but will make the system more nonlinear. This behavior, contrary to the usual effects of damping, merits further investigation. To make sense of these results, the effect of dashpot damping should be examined more closely over a wider range of frequencies, with particular attention given to the effect before, during, and after resonance.

## CONCLUSION

This work seeks to develop comprehension of a system with multiple sources of nonlinearity. To do so, this system, consisting of an overhead power transmission line with attached Stockbridge dampers undergoing vortex-induced vibrations, is modeled and analyzed. The model is represented by a system of coupled nonlinear equations that incorporate nonlinearity from all three components: mid-plane stretching from the conductor, cubic stiffness from the damper, and the oscillation of the vortex-induced lift force. Once modeled, this system is discretized using the Galerkin method. Then, using the numerical continuation method, the frequency-amplitude relation of this system at steady-state is generated. The utilized methodology is validated through comparison of natural frequencies to previous works and comparison of continuation-generated steady-state response to a direct numerical solution of the discretized equations.

To gain insight into a specific case of a conductor with a single Stockbridge damper under the lock-in condition of primary resonance, parametric analysis is employed. Using the model described above, the effect of selected system variables on the system's frequency-amplitude relation is determined. It is found that damper effectiveness increases as the damper position moves away from the conductor end, as the damper's hanging mass increases, and as the dashpot damping decreases. Furthermore, it is shown that the system's nonlinearity decreases with increasing damper position and dashpot damping. Altering the in-span damper mass within a small range is found to shift the response frequency, but not to affect amplitude or nonlinearity.

These results shed light on the fundamental properties of this coupled nonlinear system, providing a foundation for future research on the interaction between these three sources of nonlinearity. The data from the performed parametric studies can be used and expanded to optimize a damper for power lines under wind-induced vibration, while the nonlinear model of the system itself serves as an excellent base for future study using perturbation methods.

## ACKNOWLEDGMENT

This work is funded by National Science Foundation CAREER Award ECCS 1944032: Towards a Self-Powered

Autonomous Robot for Intelligent Power Lines Vibration Control and Monitoring. Any opinions, findings, and conclusions or recommendations expressed in this material are those of the author(s) and do not necessarily reflect the views of the National Science Foundation.

## CONFLICT OF INTEREST

The authors declare that they have no conflict of interest.

## REFERENCES

- [1] Skop, R. A., and Balasubramanian, S., 1997. “A new twist on an old model for vortex-excited vibrations”. *Journal of Fluids and Structures*, **11**(4), p. 395–412.
- [2] Chan, J., et al., 2009. *EPRI Transmission Line Reference Book: Wind-Induced Conductor Motion*. Electric Power Research Institute, Palo Alto, CA.
- [3] Barry, O., Zu, J. W., and Oguamanam, D. C. D., 2015. “Analytical and experimental investigation of overhead transmission line vibration”. *Journal of Vibration and Control*, **21**(14), pp. 2825–2837.
- [4] Barry, O., Oguamanam, D. C., and Lin, D. C., 2013. “Aeolian vibration of a single conductor with a stockbridge damper”. In *Proceedings of the Institution of Mechanical Engineers, Part C: Journal of Mechanical Engineering Science*, Institution of Mechanical Engineers, pp. 935–945.
- [5] Barry, O., Long, R., and Oguamanam, D. C., 2016. “Simplified vibration model and analysis of a single-conductor transmission line with dampers”. In *Proceedings of the Institution of Mechanical Engineers, Part C: Journal of Mechanical Engineering Science*, Vol. 231, Institution of Mechanical Engineers, pp. 4150–4162.
- [6] Barry, O., Zu, J. W., and Oguamanam, D. C. D., 2014. “Forced vibration of overhead transmission line: Analytical and experimental investigation”. *Journal of Vibration and Acoustics*, **136**(4).
- [7] Oliveira, A. R. E., and Freire, D. G., 1994. “Dynamical modelling and analysis of aeolian vibrations of single conductors”. *IEEE Transactions on Power Delivery*, **9**(3), pp. 1685–1693.
- [8] Verma, H., and Hagedorn, P., 2005. “Wind induced vibrations of long electrical overhead transmission line spans: a modified approach”. *Wind and Structures*, **8**(2), pp. 89–106.
- [9] Schäfer, B., 1984. “Dynamical modelling of wind-induced vibrations of overhead lines”. *International Journal of Non-Linear Mechanics*, **19**(5), pp. 455–467.
- [10] Kraus, M., and Hagedorn, P., 1991. “Aeolian vibrations: wind energy input evaluated from measurements on an energized transmission line”. *IEEE Transactions on Power Delivery*, **6**(3), pp. 1264–1270.
- [11] Nigol, O., and Houston, H. J., 1985. “Aeolian vibration of single conductor and its control”. *IEEE Transactions on Power Delivery*, **104**(11), pp. 3245–3254.
- [12] Tompkins, J. S., Merrill, L. L., and Jones, B. L., 1956. “Quantitative relationships in conductor vibration using rigid models”. *IEEE Transactions on Power Apparatus Systems*, **75**(11), pp. 879–894.
- [13] Rawlins, C. B., 1958. “Recent developments in conductor vibration”. *Alcoa Technical Paper No. 13*.
- [14] Dowell, E. H., 1980. “Component mode analysis of nonlinear and nonconservative systems”. *Journal of Applied Mechanics*, **47**(1), p. 172–176.
- [15] Pakdemirli, M., and Nayfeh, A. H., 1994. “Nonlinear vibrations of a beam-spring-mass system”. *Journal of Vibration and Acoustics*, **116**(4), p. 433–439.
- [16] Barry, O., Oguamanam, D. C. D., and Zu, J. W., 2014. “Nonlinear vibration of an axially loaded beam carrying multiple mass-spring-damper systems”. *Nonlinear Dynamics*, **77**, pp. 1597–1608.
- [17] Bukhari, M., and Barry, O., 2017. “Nonlinear vibrations analysis of overhead power lines: A beam with mass-spring-damper-mass systems”. *Journal of Vibration and Acoustics*, **140**(3).
- [18] Sarpakaya, T., 1979. “Vortex-induced oscillations: a selective review”. *Journal of Applied Mechanics*, **46**, p. 241–258.
- [19] Griffin, O. M., and Ramberg, S. E., 1982. “Some recent studies of vortex shedding with application to marine tubulars and risers”. *ASME Journal of Energy Resources Technology*, **104**, p. 2–13.
- [20] Parkinson, G., 1989. “Phenomena and modeling of flow-induced vibrations of bluff bodies”. *Progress in Aerospace Sciences*, **26**, p. 169–224.
- [21] Pantazopoulos, M. S., 1994. “Vortex-induced vibration parameters: critical review”. In *Proceedings International Conference on Offshore Mechanics and Arctic Engineering*, Vol. 1, pp. 199–255.
- [22] Kim, W.-J., and Perkins, N. C., 2002. “Two-dimensional vortex-induced vibration of cable suspensions”. *Journal of Fluids and Structures*, **16**(2), p. 229–245.
- [23] Hartlen, R. T., and Currie, I. G., 1970. “Lift-oscillator model of vortex-induced vibration”. *Journal of the Engineering Mechanics Division*, **96**(5), p. 577–591.
- [24] Skop, R. A., and Griffin, O. M., 1973. “A model for the vortex-excited resonant response of bluff cylinders”. *Journal of Sound and Vibration*, **27**(2), p. 225–233.
- [25] Iwan, W. D., and Blevins, R. D., 1974. “A model for

- vortex induced oscillation of structures”. *Journal of Applied Mechanics*, **41**(3), p. 581–586.
- [26] Skop, R. A., and Griffin, O. M., 1974. “On a theory for the vortex-excited oscillations of flexible cylindrical structures”. *Journal of Sound and Vibration*, **41**, p. 263–274.
- [27] Iwan, W. D., 1975. “The vortex induced oscillation of elastic structural elements”. *ASME Journal of Engineering for Industry*, **97**, p. 1378–1382.
- [28] Ramberg, S. E., and Griffin, O. M., 1974. “Vortex formation in the wake of a vibrating, flexible cable”. *ASME Journal of Fluids Engineering*, **96**, p. 317–322.
- [29] Ramberg, S. E., and Griffin, O. M., 1976. “Velocity correlation and vortex spacing in the wake of a vibrating cable”. *ASME Journal of Fluids Engineering*, **99**, p. 10–18.
- [30] Barry, O., Long, R., and Oguamanam, D. C. D., 2017. “Rational damping arrangement design for transmission lines vibrations: Analytical and experimental analysis”. *Journal of Dynamic Systems, Measurement, and Control*, **139**(5).
- [31] Bukhari, M. A., Barry, O., and Tanbour, E., 2017. “On the vibration analysis of power lines with moving dampers”. *Journal of Vibration and Control*.